

NONLINEAR PARTIAL DIFFERENTIAL EQUATIONS IN ENGINEERING AND APPLIED SCIENCE

Proceedings of a Conference Sponsored By
Office of Naval Research

Held At

University of Rhode Island
Kingston, Rhode Island

edited by

ROBERT L. STERNBERG

Office of Naval Research
Boston, Massachusetts

ANTHONY J. KALINOWSKI

Naval Underwater Systems Center
New London, Connecticut

JOHN S. PAPADAKIS

University of Rhode Island
Kingston, Rhode Island

COPYRIGHT © 1980 by MARCEL DEKKER, INC.

MARCEL DEKKER, INC.

New York and Basel

A SINGULARITY THEORY APPROACH TO
STEADY-STATE BIFURCATION THEORY

Martin Golubitsky and David Schaeffer

Arizona State University
Tempe, Arizona

and

Duke University
Durham, North Carolina

§1. INTRODUCTION

In this article we describe how the singularity theory of mappings can be used to help solve problems in steady-state bifurcation theory. Most of the results which follow have appeared or will appear elsewhere; our objective here is to explain rather than to prove.

We consider two theoretical issues:

- A. Solve $G(x, \lambda) = 0$ where $x = (x_1, \dots, x_n) \in \mathbb{R}^n$ and $\lambda \in \mathbb{R}$ are near 0 and $G(x, \lambda) = (g_1(x, \lambda), \dots, g_n(x, \lambda))$ is C^∞ .
- B. Find all small C^∞ perturbations of the zero set $G = 0$.

Before analyzing specific examples, we would like to make some general comments. The situation which we visualize in A is that G is given either explicitly by some system of ordinary differential equations $\dot{x} = G(x, \lambda)$ depending smoothly on the parameter λ or implicitly by reduction from some infinite dimensional operator by a procedure like that of Lyapunov and Schmidt. The variables x are internal state variables and the variable λ is external, being varied quasistatically by some experimenter. In particular, we are interested in the number (and stability) of solution x to A for each fixed λ as λ varies from negative to positive through zero. Thus, it does not matter whether we find the zero set of the given G or whether we find the zero set of any H containing the same information.

Practically, the simplest way to preserve the zero set is through smooth changes of coordinates. (We note that the coordinate changes that we have in mind will not in general preserve the stability of solutions. However, for the applications which we describe here the stability of solutions may be assigned a posteriori.)

Definition 1 Two bifurcation problems G and H are contact equivalent if

$$H(x, \lambda) = T(x, \lambda)G(X(x, \lambda), \Lambda(\lambda))$$

where $X(0,0) = 0$, $\Lambda(0) = 0$, $\det (d_x X)_{(0,0)} > 0$, $\Lambda_\lambda(0) > 0$, and for each (x, λ) near $(0,0)$, $T(x, \lambda)$ is an invertible $n \times n$ matrix.

It should be clear that T does not affect the zero set while $\zeta(x, \lambda) = (X, \Lambda)$ is just an (orientation preserving) change of coordinates. The assumption that Λ does not depend on x guarantees that the number of solutions as λ varies through zero will remain the same in the new coordinate system. We assume that ζ is C^∞ as the main theorems are proved with this hypothesis. However, it is sufficient for the applications that ζ be only a homeomorphism. We call this more general situation C^0 contact equivalence.

For a given application (and thus a given G) our approach to A will be to prove the existence of a contact equivalence of G to a new and simpler problem H (called a normal form) and then solve $H = 0$.

The importance of B is clear. If one performs an experiment whose steady states are idealized by the mathematical problem $G = 0$, then one will actually measure $H = 0$ where--if the model is a good one-- H is a small perturbation of G . Thus, one would like to classify all small perturbations of G --at least up to contact equivalence. Mathematically, this is done through the notion of a universal unfolding. We shall give several examples of this method in subsequent sections. For the moment, one should observe that what is meant by "all small perturbations" may actually vary from example to example. In particular, many idealized physical problems are given along with a group of symmetries. In many of these cases one is only interested in those perturbations which maintain the given group of symmetries.

The specific examples which we consider are: (a) buckling of a Euler column [6]; (b) bifurcation in continuous flow stirred tank reactors (this is joint work with Barbara Keyfitz [4]); (c) mode jumping in the buckling of a rectangular plate [12]; and (d) recent work on the problem of thermal convection in spherical geometry [9].

Other examples where our theory has proved helpful are: (e) analysis of bifurcation near a double eigenvalue in the "Brusselator" [13] (which is a much studied model reaction diffusion equation); (f) an analysis of boundary effects in the Taylor problem in hydrodynamic stability [11]; and (g) an explanation for the existence of an explosion peninsula in the combustion of hydrogen and oxygen [5] (which is again joint work with Barbara Keyfitz).

§2. BUCKLING OF A EULER STRUT

Consider the strut pictured in Fig. 1. Let $\lambda + \lambda_0$ be the applied load where λ_0 is the critical load where buckling first occurs. The variable x represents, for pedagogical purposes, the maximum deviation of the strut from the horizontal. Let $V(x, \lambda)$ be the potential energy of the strut; then (for x and λ scaled) we have that

$$G(x, \lambda) = \frac{\partial V}{\partial x}(x, \lambda) = x^3 - \lambda x + \dots \quad (1)$$

defines the steady state configurations on the strut. (See [6], Sec. 6, for details.)

The issues raised in the Introduction are solved for this example by the following:

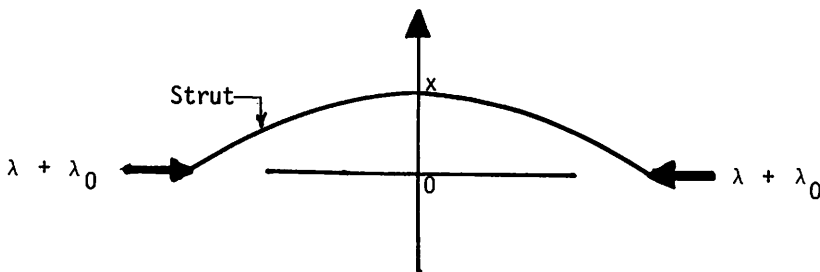


FIG. 1. Buckling of a Euler strut.

Proposition 1

- (a) G in (1) is contact equivalent to $x^3 - \lambda x$.
 (b) $F(x, \lambda, \alpha, \beta) = x^3 + \beta x^2 - \lambda x + \alpha$ is a universal unfolding of $x^3 - \lambda x$.

The first part of this proposition shows that one may neglect the higher order terms in (1). Thus the zero set of G in (1) is--up to a smooth change of coordinates--just the familiar pitchfork pictured in Fig. 2.

The content of part (b) of Proposition 1 is that any small perturbation of (1) may be found up to contact equivalence in the family F for some fixed α and β . Actually more is proved as the choice of α and β depend smoothly on the perturbation.

The information about bifurcation diagrams contained in F may be organized [6,8] to show that all small perturbations of the pitchfork are pictured, up to a smooth change of coordinates, in Fig. 3. (For a more precise statement of the information contained in Fig. 3, see [6].)

A final observation is that the universal unfolding parameters depend nonsingularly on the physical parameters a and b where a is a central load and b is an initial unstressed curvature. See Fig. 4. The pitchfork is actually richer in structure than one might think at first.

Definition 2 The minimum number of parameters to appear in a universal unfolding of a given problem G is called the codimension of G .

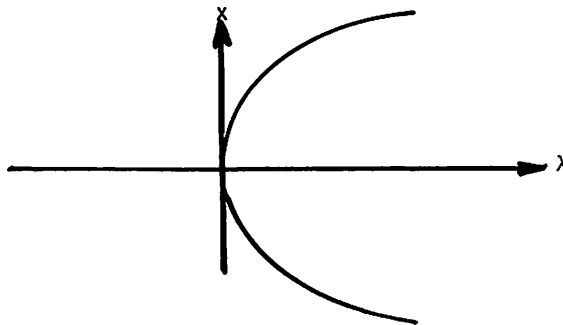


FIG. 2. The pitchfork. Organizing center for Euler buckling.

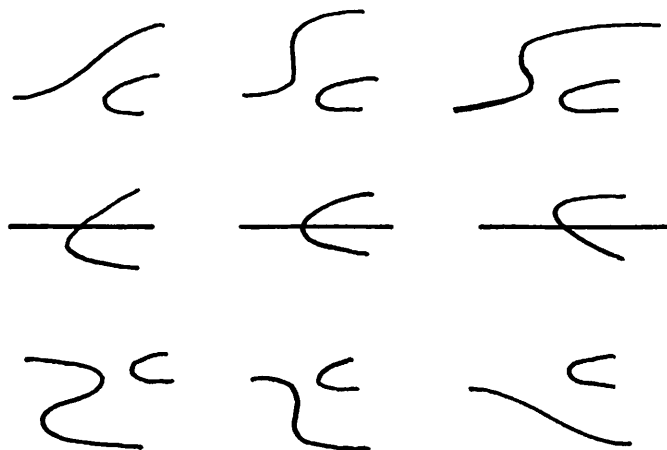


FIG. 3. Classification of perturbations of the pitchfork.

As indicated above the pitchfork $x^3 - \lambda x$ has codimension two.

An easy to misapply maxim, motivated by geometric considerations in singularity theory, is that in a physical model one expects to observe only problems which are stable under small perturbations; that is, problems of codimension zero. The loose reasoning is simply that the mathematical description of a physical problem should have the same form when subjected to small perturbations or else it will not be observed. This naive reasoning fails in many ways (for discussions, see [3,7]); however, it is useful as a warning. In particular, it suggests questioning why (the mathematical idealization of) Euler buckling generates a bifurcation problem of codimension two.

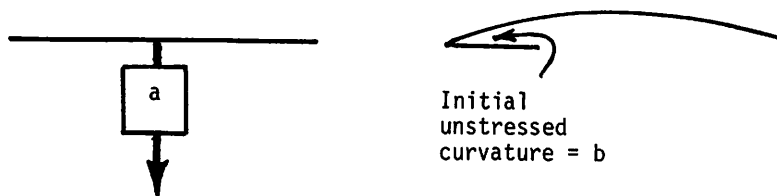


FIG. 4. Physical imperfections in Euler buckling.

The answer is simple: symmetry. Models for Euler buckling assume that "buckling up" has the same potential energy as "buckling down." Thus V is forced to be even in x and G odd in x .

A universal unfolding of the pitchfork $x^3 - \lambda x$ in the space of all functions which are odd in x contains zero parameters [7]. In other words, if $H(x, \lambda)$ is a small perturbation of $x^3 - \lambda x$ which is odd in x , then H is contact equivalent to the pitchfork.

§3. THE CONTINUOUS FLOW STIRRED TANK REACTOR

A continuous flow stirred tank reactor (CSTR) is an idealized and simplified chemical reactor which chemical engineers have found useful. Uppal, Ray, and Poore [15] studied the steady states of the CSTR by a combination of analytic techniques and computer calculations. In joint work with Barbara Keyfitz [4] it was shown that Uppal et al. had found most, but not all, of the qualitative behavior which can be exhibited by a CSTR. Interestingly, the study of this problem from the singularity theory point of view led to a more singular bifurcation problem than those studied in classical bifurcation theory. Recent work [5] on aspects of the combustion of hydrogen and oxygen shows the necessity of studying a yet more degenerate bifurcation problem. It seems likely that chemical reaction problems, with their large number of external parameters, will yield examples of bifurcation problems which are as complicated as the most complicated examples which mathematics can analyze.

Consider Fig. 5 which gives a schematic diagram for a CSTR. A reactant flows in and out of the reactor with flow rate ϵ . One measures two states of the reactor, the internal temperature y and the concentration of the reactant x . The simplifying assumption that the reactor is continuously stirred implies that x and y are uniform throughout the interior. The ambient temperature is η and one assumes that the reactant enters the reactor with concentration 1 and (scaled) temperature 0. (The temperature is also scaled so that -1 is absolute zero.)

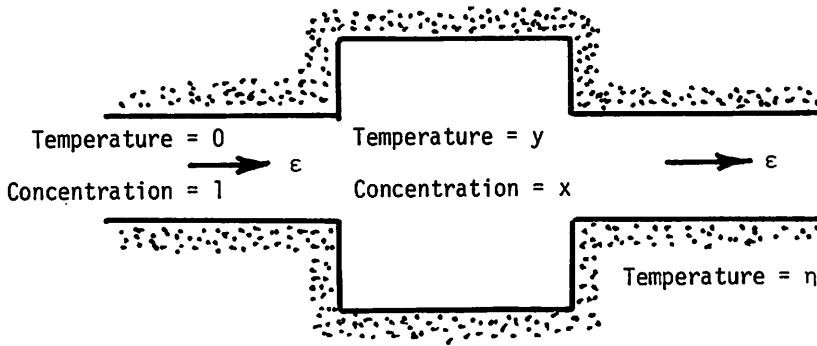


FIG. 5. Schematic diagram of a CSTR.

The ordinary differential equations describing the time dependence of x and y (in nondimensionalized form) are:

$$\begin{aligned} \frac{dx}{dt} &= \epsilon - \epsilon x - \frac{1}{\delta} A(y) \\ \frac{dy}{dt} &= -\epsilon y - (y - \eta) + \frac{B}{\delta} A(y) \end{aligned} \tag{2}$$

where

$$A(y) = \exp(\gamma y / (y + 1)) \tag{3}$$

is the temperature dependent reaction rate in Arrhenius form. The remaining constants measure physical characteristics of the reactant and the tank. More precisely, γ is the activation energy (usually thought to be between 5 and 20), δ is a Damköhler number measuring the ratio of heat loss across the wall to chemical heat gain, and B measures adiabatic heat gain.

The bifurcation problem for the CSTR is posed as follows: How do the steady states of this system evolve as the flow rate ϵ is varied quasistatically while B , δ , γ , and η (which are properties of a particular reactor) are held fixed? Can one classify the qualitative nature of the various bifurcation diagrams up to smooth changes of coordinates?

Observe that when setting the right-hand side of (2) to zero, one may eliminate x to obtain the following equation for the steady states:

$$G(y, \epsilon, B, \delta, \eta) = \eta - (1 + \epsilon)y + \frac{B\epsilon}{1 + \epsilon\delta A(y)} = 0 \tag{4}$$

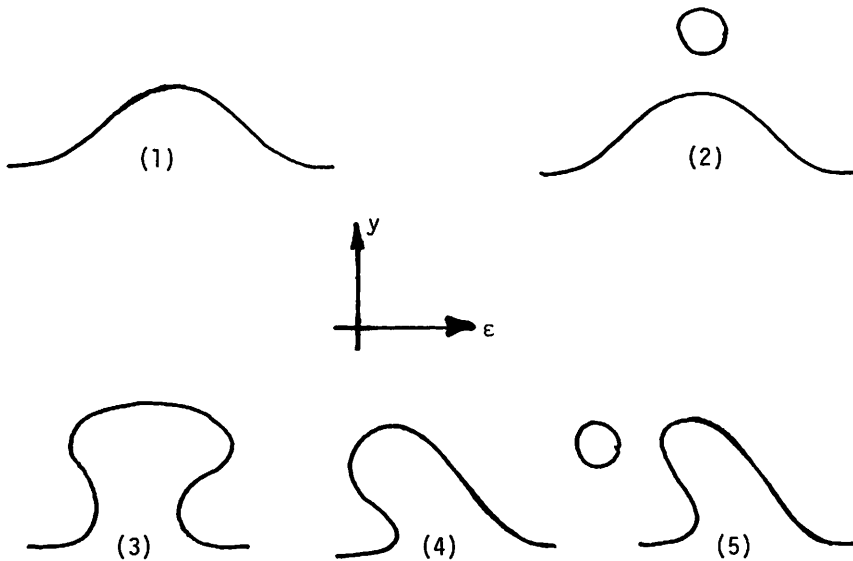


FIG. 6. Qualitative types of bifurcation diagrams found by Uppal, Ray, and Poore [15].

where $\Lambda(y) = 1/A(y)$. Thus for fixed B, δ, η the bifurcation diagrams may be drawn in the $y\epsilon$ plane. Uppal et al. [15] found five types of bifurcation diagrams which are pictured in Fig. 6.

We observe that these diagrams are all small perturbations of a simple singular bifurcation problem $x^3 + \lambda^2 = 0$ which we call the winged cusp (see Fig. 7). The following proposition makes this observation more precise.

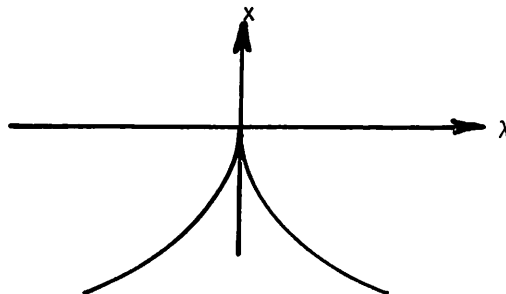


FIG. 7. The winged cusp; organizing center for the CSTR.



FIG. 8. Additional perturbations of the winged cusp.

Proposition 2

- (a) A universal unfolding for $x^3 + \lambda^2$ is given by

$$F(x, \lambda, \alpha_1, \alpha_2, \alpha_3) = x^3 - (\alpha_2 \lambda + \alpha_3)x + \lambda^2 + \alpha_1$$
- (b) There are seven stable bifurcation diagrams contained in F (for fixed $\alpha_1, \alpha_2, \alpha_3$) up to smooth changes of coordinates. They are the five found by Uppal et al. [15] plus the two given in Fig. 8.

This proposition suggests that the winged cusp should appear in (4) for some fixed value of B, δ, η . In fact one can prove [4]:

Theorem 1 For all $\gamma > 8/3$

- (a) There exists a unique choice (B_0, δ_0, η_0) and a unique (y_0, ϵ_0) such that $G(y, \epsilon, B_0, \delta_0, \eta_0)$ is contact equivalent (on a small neighborhood) of (y_0, ϵ_0) to the winged cusp $x^3 + \lambda^2$.
- (b) The universal unfolding parameters $\alpha_1, \alpha_2, \alpha_3$ depend nonsingularly on the physical parameters B, δ, η .
- (c) The local bifurcation behavior which occurs in (4) already appears (up to contact equivalence) in the universal unfolding of the winged cusp.

This theorem makes it reasonable to call the winged cusp the organizing center for the steady states in the CSTR.

We end this section with a comparison of the CSTR with the Euler strut. It may seem surprising that one of the non-stable bifurcation diagrams which occurs in the universal unfolding of the winged cusp is the pitchfork--only as pictured in Fig. 9. To see this set $\alpha_1 = \alpha_2 = 0$ and $\alpha_3 > 0$.



FIG. 9. The pitchfork as a perturbation of the winged cusp.

The question we ask is: Why is the pitchfork so central to the understanding of the steady-state structure of the buckling of an Euler strut and yet so unimportant in the CSTR that the people who have analyzed the CSTR previously had not even noted its existence? The answer, again, seems to be symmetry; there is no natural reflectional symmetry present in the CSTR.

§4. MODE JUMPING IN BUCKLING OF RECTANGULAR PLATES

Consider the rectangular plate of Fig. 10. It is well known that when such a plate is buckled it can support a number of configurations. These configurations are distinguished by their wave number, by which we mean the number of zeroes of the normal deflection function along a line parallel to the sides.

Experiments by Manuel Stein [14] show that mode jumping for such a plate can occur. More precisely, Stein considers a plate where the aspect ratio ℓ is approximately 5.38 and finds that the plate first buckles into a configuration with wave number 5. Moreover, when the load λ is increased to approximately 1.7 times the initial loading, the plate jumps "suddenly" and "violently" into a configuration with wave number 6. It is this secondary buckling which is termed mode jumping.

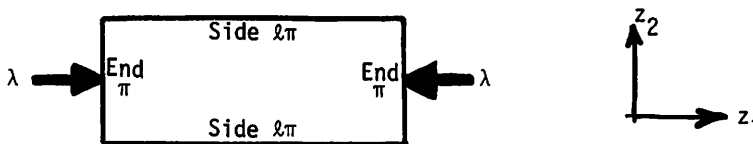


FIG. 10. Buckling of a rectangular plate.

In fact, as λ is increased further buckled states with wave numbers 7 and 8 appear. However, these states occur after the plate has begun to deform plastically. We only consider elastic deformations and will attempt to explain the jump from 5 to 6 buckles by analyzing the von Kármán equations.

There are several commonly used boundary conditions associated with the von Kármán equations. We find that whether or not mode jumping occurs by our methods, depends on which boundary conditions are employed. Fortunately, when one uses the boundary conditions which are most relevant for Stein's [14] experiment, one does obtain a mathematical explanation for mode jumping.

The von Kármán equations are:

$$\begin{aligned} \Delta^2 w &= [\phi, w] - \lambda w_{z_1 z_1} \\ \Delta^2 \phi &= -\frac{1}{2} [w, w] \end{aligned} \tag{5}$$

where w is the vertical deflection function (in the z_3 direction), ϕ the Airy stress function, and Δ^2 the biharmonic operator, and

$$[u, v] = u_{z_2 z_2} v_{z_1 z_1} - 2u_{z_1 z_2} v_{z_1 z_2} + u_{z_1 z_1} v_{z_2 z_2}$$

It is somewhat difficult to determine completely realistic boundary conditions for Stein's experiment. We consider the following boundary conditions for ϕ :

$$\phi_N = (\Delta\phi)_N = 0 \quad \text{on boundary} \tag{6}$$

where N indicates differentiation in the direction normal to the boundary. This differs from the case most frequently studied, namely, $\phi = \Delta\phi = 0$ on the boundary. We explain this choice in [12]. There are two choices of boundary conditions for w which are often employed: clamped and simply supported.

$$\left. \begin{aligned} w = w_N = 0 & \quad \text{on ends} \\ w = \Delta w = 0 & \quad \text{on sides} \end{aligned} \right\} \text{ (clamped)} \tag{7a}$$

$$w = \Delta w = 0 \quad \text{on boundary} \quad \text{(simply supported)} \tag{7b}$$

Stein, in his paper [14], suggests that clamped boundary conditions are more appropriate for his experiment; indeed, the difficulties of achieving simply supported boundary conditions in practice are well known. However, many mathematicians have frequently studied simply supported boundary conditions, presumably to facilitate computations. In Sec. 2 of [12], we give a more detailed discussion of the merits of various boundary conditions. In any case, for comparison we consider both choices of boundary conditions.

In [1], Bauer, Keller, and Reiss suggest that mode jumping should be thought of as a secondary bifurcation and that secondary bifurcations are created by perturbing double eigenvalues. The double eigenvalues are obtained as follows: Consider the linearized von Karman equation

$$\Delta^2 w + \lambda w_{z_1 z_1} = 0 \quad (8)$$

with the two choices of boundary conditions. One finds that for a discrete set of values, ℓ_0 of the aspect ratio ℓ , the first eigenvalue [in (8)] is double. In particular, the critical aspect ratios and the corresponding eigenfunctions are

$$\begin{aligned} \ell_0 &= \sqrt{k(k+2)} \\ w_1 &= \left[\frac{k+2}{k} \sin\left(\frac{kz_1}{\ell}\right) - \sin\left(\frac{k+2}{\ell} z_1\right) \right] \sin(z_2) \end{aligned} \quad (9a)$$

$$w_2 = \left[\cos\left(\frac{kz_1}{\ell}\right) - \cos\left(\frac{k+2}{\ell} z_1\right) \right] \sin(z_2)$$

$$\begin{aligned} \ell_0 &= \sqrt{k(k+1)} \\ w_1 &= \sin\left(\frac{k}{\ell} z_1\right) \sin(z_2) \\ w_2 &= \sin\left(\frac{(k+1)}{\ell} z_1\right) \sin(z_2) \end{aligned} \quad (9b)$$

for clamped and simply supported boundary conditions, respectively. Note that wave numbers of 5 and 6 occur at a double eigenvalue when $\ell_0 = \sqrt{35} = 5.92$ for clamped conditions, and $\ell_0 = \sqrt{30} = 5.48$ for simply supported boundary conditions.

In either case the actual experimental ℓ of 5.38 is slightly less than the critical ℓ_0 where a double eigenvalue occurs.

The classical Lyapunov-Schmidt, essentially the implicit function theorem for Banach spaces, guarantees the existence of a smooth mapping.

$$G : \mathbb{R}^2 \times \mathbb{R} \rightarrow \mathbb{R}^2$$

where $G(x,y,\lambda) = (g_1(x,y,\lambda), g_2(x,y,\lambda))$ (10)

such that $G = 0$ parametrizes the solution to the full nonlinear von Kármán equations. Here $xw_1 + yw_2$ parametrize the eigenspace to (8) at the double eigenvalue where w_1 and w_2 are given by (9).

Observe now that there are several reflectional symmetries present in this problem. As with the Euler strut, one assumes implicitly in the von Kármán equations that buckling up has the same potential energy as buckling down. Reflecting about the center line connecting the sides of the plate also preserves the solution set. These two symmetries induce restrictions on G in (10). In particular, g_1 must be odd in x and even in y , while g_2 is odd in y and even in x . Thus, to the lowest order G must have the form

$$G(x,y,\lambda) = (ax^3 + bxy^2 - \lambda x, cx^2y + dy^3 - \lambda y) + \dots \quad (11)$$

when the aspect ratio is as in (9). For the von Kármán equations $a \cdot d$ is positive; thus, scaling implies that G has the form

$$G(x,y,\lambda) = (x^3 + bxy^2 - \lambda x, cx^2y + y^3 - \lambda y) + \dots \quad (12)$$

Definition 3 A bifurcation problem (12) is nondegenerate if

- (a) $g_1 = 0$ and $g_2 = 0$ are nowhere tangent
- (b) The cubic parts of g_1 and g_2 have no common factors

The main results from singularity theory are:

Theorem 2 Let G be a nondegenerate bifurcation problem of type (12). Then

- (a) The higher order terms in (12) can be removed by a contact equivalence

- (b) A universal unfolding of (12) preserving the given symmetries contains one new parameter and is given by

$$F(x, y, \lambda, b, c, L) = (x^2 + bxy^2 - \lambda x, cx^2y + y^3 - (\lambda - L)y) \quad (13)$$

Setting $L = 0$, one observes that degeneracies occur when $b = 1$, $c = 1$, and $bc = 1$. These curves separate the bc -plane into seven regions as shown in Fig. 11. One can prove more: (b, c) and (b', c') are in the same region of the bc -plane if and only if G and $G' = (x^2 + b'xy^2 - \lambda x, c'x^2y + y^3 - \lambda y)$ are C^0 contact equivalent.

Using the Lyapunov-Schmidt method, one can actually compute b and c at the aspect ratios ℓ_0 in (9) obtaining:

Theorem 3

- (a) For clamped boundary conditions the point (b, c) lies in region 4 of Fig. 11
- (b) For simply supported boundary conditions the point (b, c) lies in region 1 of Fig. 11
- (c) For either choice of boundary conditions the unfolding parameter L can be identified with the aspect ratio $\ell - \ell_0$

If one studies the bifurcation diagrams associated with (13) when $L < 0$, one sees that the assumption of simply supported boundary conditions can not lead to mode jumping, at least by these methods, while clamped boundary conditions do lead to mode jumping.

In particular, if (b, c) lies in region 1 of Fig. 11 then the associated bifurcation diagram is shown in Fig. 12. Observe that after the initial bifurcation the solution lies on branch (d) and no secondary bifurcation occurs. (Branch (d) corresponds to solutions with wave number 5.) If (b, c) lies in region 4, the associated bifurcation diagram is pictured in Fig. 13.

Now after the initial bifurcation to branch (d) there is a secondary bifurcation which causes a jump to branch (c). (Branch (c) corresponds to solutions with wave number 6.)

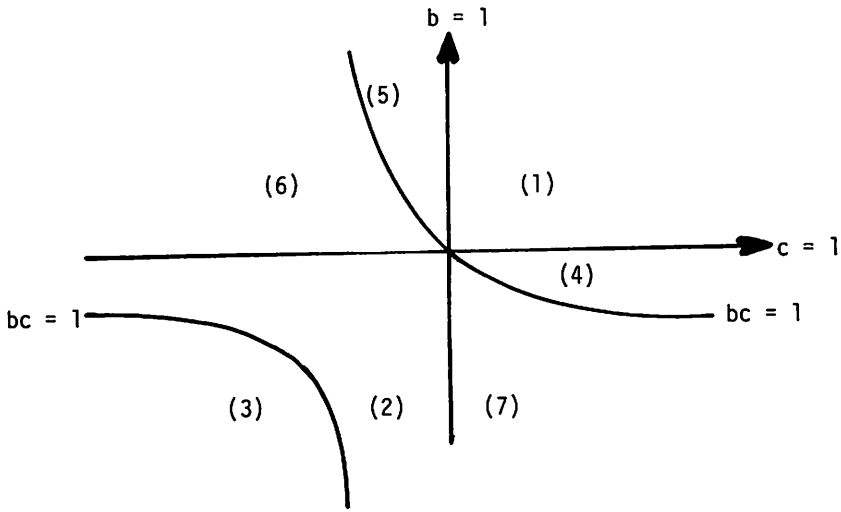


FIG. 11. Degeneracies of (12) viewed in the modal parameter plane.

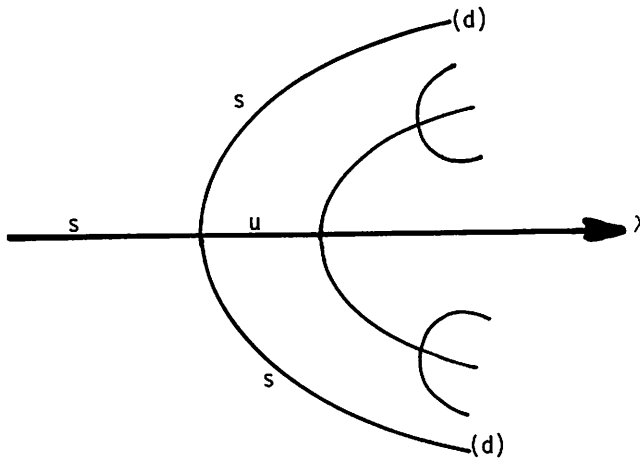


FIG. 12. Perturbations of region 1 with simply supported boundary conditions.

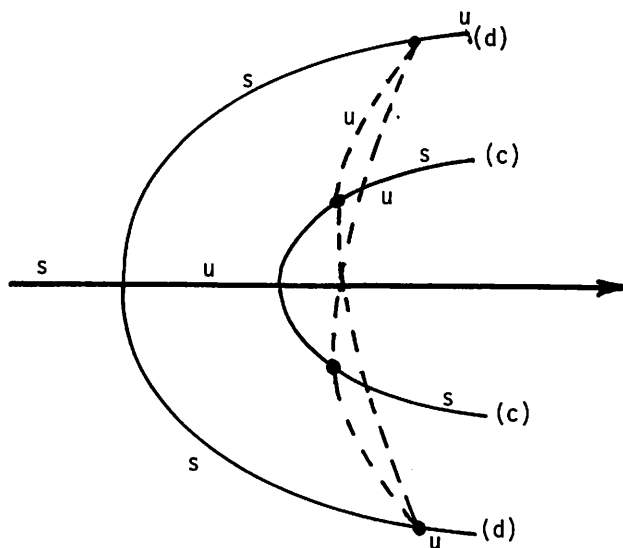


FIG. 13. Perturbations of region 4 with clamped boundary conditions.

§5. THE BÉNARD PROBLEM IN A SPHERICAL GEOMETRY

The language of singularity theory can be very helpful in organizing experimental data by relating them to known theoretical results. As an illustration of this power, we consider the Bénard problem in a spherical geometry, a problem which arises in plate tectonics. This problem has been considered by, among others, Chossat [2] from a theoretical point of view and Young [16] in a numerical simulation. Chossat considers the self-adjoint case (defined below); he shows that in this case the only bifurcating solutions are axisymmetric and that they appear supercritically. Young, on the other hand, considers a nonself-adjoint case, and in his data non-axisymmetric solutions play an important role. In the process of trying to reconcile this disparate information one is led to a rather convincing plausibility argument that the basic bifurcation in the case Young considers must be subcritical, a point on which he makes no comment. Of course, this involves no contradiction, as he considers a nonself-adjoint case. Nevertheless, it is a little surprising that a seemingly small change in certain auxiliary parameters can reverse the orientation of the primary bifurcation in this problem.

It should be remarked that the complexity of the problem renders a direct analysis exceedingly difficult; for example, the calculations of Young required integration of a time-dependent system of nonlinear equations with nontrivial dependence on all three space coordinates.

The governing equations for this problem are formulated on a three-dimensional annular region

$$\Omega = \{x \in \mathbb{R}^3 : \eta < |x| < 1\} \quad (14)$$

where $\eta = 0.3$. Both authors work in the Boussinesq approximation. After subtraction of the conduction solution, the equations become

$$u_t = -\nabla p + \Delta u + R\vec{g}(r)\theta - (u \cdot \nabla)u \quad (15a)$$

$$\theta_t = \frac{1}{P} (\Delta\theta + R \nabla T_0 \cdot u) - (u \cdot \nabla)\theta \quad (15b)$$

Here u , p , and θ measure velocity, pressure, and temperature, respectively, while P and R are the Prandtl and Rayleigh numbers, respectively. The gravity vector $\vec{g}(r)$ is given by

$$\vec{g}(r) = \frac{\gamma_1}{r^3} \vec{r} + \gamma_2 \vec{r}$$

and

$$\nabla T_0 = \frac{\beta_1}{r^3} \vec{r} + \beta_2 \vec{r}$$

is the gradient of the equilibrium temperature. (More detail concerning the origin of (15) is given in both [2] and [16].) If $\gamma_1/\gamma_2 = \beta_1/\beta_2$, then Eq. (15) linearized about the zero solution defines a self-adjoint operator; intuitively, this just means that θ enters into the u equation (15a) in the same form that u enters into the θ equation (15b).

The zero solution of (15) loses stability as the Rayleigh number R is increased, and nontrivial steady-state solutions bifurcate from the trivial solution. In studying these bifurcations we make three reductions of the problem, starting with the standard Lyapunov-Schmidt procedure. Let v_i , $i = 1, \dots, n$ be a basis for the kernel of the linearization of (15) at the

first bifurcation point, say at $R = R_c$. This reduction is based on looking for a solution u of (15) in the form

$$u = \sum_{i=1}^n x_i v_i + W(x, \lambda) \quad (16)$$

where $\langle v_i, W \rangle = 0$ and $\lambda = R - R_c$. (Here x denotes the n -vector of unknown coefficients in (16), not a spatial coordinate.) The method leads to a parametrization of solutions of (15) by the solutions of a certain $n \times n$ system of equations

$$G(x, \lambda) = 0 \quad (17)$$

In principle, derivatives of any order of the reduced mapping $G : \mathbb{R}^n \times \mathbb{R} \rightarrow \mathbb{R}^n$ may be calculated at the origin from (15) in the standard way (see [2] for details).

For the problem at hand with $\eta = 0.3$ in (14), calculations show that the first bifurcation from (15) is from an eigenvalue of multiplicity 5. Indeed, this bifurcation provides an instance of high multiplicity occurring as a result of symmetry, as described by Sattinger [10]. Specifically, Eq. (15) is invariant under the action of the orthogonal group $O(3)$. The high multiplicity arises as follows. An axisymmetric bifurcating solution of (15) may be found, and it has the angular dependence of the spherical harmonic $Y_{20}(\theta, \phi)$. Because of the invariance of (15), any rotation operator applied to this function will yield another solution. Of course, the kernel of the linearized problem is a linear subspace, and the linear span of the set of rotations of $Y_{20}(\theta, \phi)$ is five-dimensional, a basis being provided by $\{Y_{2m}(\theta, \phi), m = -2, \dots, 2\}$. The action of $O(3)$ on Eq. (15) leads to an irreducible representation of $O(3)$ on the five-dimensional space spanned by $\{Y_{2m}\}$. (See [10].)

The spherical harmonics $\{Y_{2m}\}$ provide one representation of $O(3)$, but there is an isomorphic form of the representation that is more convenient for our analysis. Let X be the set of symmetric 3×3 matrices A with trace zero, and consider the representation π of $O(3)$ defined by

$$\pi(S)A = SAS^{-1} \quad (18)$$

where $S \in O(3)$. It follows by a refinement [7] of the arguments of Sattinger [10] that the reduced mapping G may be expressed in the form

$$G(A, \lambda) = f(\text{tr } A^2, \det A, \lambda)A + g(\text{tr } A^2, \det A, \lambda)\{A^2 - \frac{1}{3}(\text{tr } A^2)I\} \quad (19)$$

Here we use coordinates on \mathbb{R}^5 such that the representation of $O(3)$ assumes the form (18). The coefficients f and g in (19) represent arbitrary invariant functions on X . The restricted form of (19) is a tremendous simplification compared to the general mapping $G : \mathbb{R}^5 \times \mathbb{R} \rightarrow \mathbb{R}^5$; indeed, this is our second reduction of the problem.

Our third reduction of the problem, from five dimensions to two, is specific to the problem at hand, unlike the preceding two which were general. Let

$$Z = \{A \in X : A \text{ is diagonal}\}$$

Then Z is a two-dimensional subspace of X (recall that X contains only matrices of trace 0) with the property that

$$\pi[O(3)] \cdot Z = X \quad (20)$$

Because of (20) it suffices to examine the reduced mapping G on Z . With respect to an appropriately chosen complex coordinate on Z , Eq. (19) assumes the form

$$G(z, \lambda) = f(|z|^2, \text{Re } z^3, \lambda)z + g(|z|^2, \text{Re } z^3, \lambda)\bar{z}^2 \quad (21)$$

where \bar{z} denotes the complex conjugate of the complex number z . This completes the reduction of the problem, which only involved singularity theory peripherally.

The singularity theory methods are used to study what coefficients in (21) are likely to occur. Using the codimension--relative to $O(3)$ --as a measure of complexity, one finds a list of cases increasing in complexity, starting as follows:

Case 0: $f(0) \neq 0$

Case 1: $f(0) = 0, g(0) \neq 0, f_\lambda(0) \neq 0$

Case 2: $f(0) = g(0) = 0$, plus nondegeneracy conditions

In the zeroth case here (21) is nonsingular; i.e., the differential dG is invertible and no bifurcation occurs. We pass over this case because we imagine setting the bifurcation parameter R to the value which produces bifurcation.

In case 1, Eq. (21) may be transformed by a contact equivalence preserving the symmetry group $O(3)$ to the very simple form

$$-\lambda z + \bar{z}^2 = 0 \quad (22)$$

The solution set of (22) consists of the trivial solution $z = 0$ and three crossed lines

$$z = \lambda e^{(2\pi i/3)j} \quad j = 0, 1, 2 \quad (23)$$

To relate these solutions with solutions of the full reduced Eq. (19), one must recall that each point $z \in Z$ generates an orbit in X when $O(3)$ acts on Z . Typically, this orbit will be three-dimensional, as $O(3)$ is a three-dimensional group. However, if z has special properties (e.g., axial symmetry) the orbit may have lower dimension (two if z has axial symmetry). It turns out that a point z in Z has axial symmetry iff z^3 is real; thus (23) consists exclusively of axisymmetric functions. Therefore, each solution (23) of (22) corresponds to a two-dimensional manifold of axisymmetric solutions of (19), the two parameters corresponding to the choice of the axis of symmetry.

Generically, one would expect case 1 to appear when bifurcation occurs; otherwise, one would have to explain why $g(0)$ or $f_\lambda(0)$ happened to vanish. However, Chossat showed that in the self-adjoint case it follows from an integration by parts that indeed $g(0) = 0$, so one is led to consider case 2. In this case the canonical form is

$$(\varepsilon|z|^2 - \lambda)z + (|z|^2 + C \operatorname{Re} z^3)\bar{z}^2 = 0 \quad (24)$$

where C is a constant which cannot be scaled away and $\varepsilon = \pm 1$. The nondegeneracy conditions required to derive (24) are as follows: Let $u = |z|^2$, $v = \operatorname{Re} z^3$ be the arguments of f and g in (21); then one must have

$$f_u(0) \neq 0 \quad f_\lambda(0) \neq 0 \quad g_u(0) \neq 0$$

Chossat also shows that the bifurcation is supercritical so that $\epsilon = +1$ is the appropriate choice in (24).

The solutions of (24) may be obtained explicitly: There is the trivial solution $z = 0$ and three curves of solutions located in planes containing the λ axis and making an angle of 120° with one another, specifically

$$\lambda = r^2 + r^3 + Cr^4 \quad z = re^{(2\pi i/3)j} \quad j = 0, 1, 2 \quad (25)$$

where $-\infty < r < \infty$. While (23) is suggestive of the familiar transcritical bifurcation from a simple eigenvalue, (25) is suggestive of supercritical bifurcation from a simple eigenvalue, with this significant difference: When $r < 0$ in (25) the corresponding solution is stable, while for $r > 0$ it is unstable. Also note that all points enumerated in (25) are axisymmetric.

As mentioned above, nonaxisymmetric solutions figured prominently in the numerical simulation of Young [16]. Specifically, Young found that the axisymmetric solution which bifurcated at Rayleigh number R_C remained stable only up to $R \approx 2.9 R_C$, while a nonaxisymmetric steady solution (still with angular dependence associated to spherical harmonics of order 2) appeared at $R \approx 2.2 R_C$ and remained stable up to the largest value of R in his data, approximately $4.5 R_C$. The most significant point here is that in the range $2.2 R_C < R < 2.9 R_C$, both the axisymmetric and nonaxisymmetric solutions are stable.

The cases considered by Young [16] and Chossat [2] differ only in the value of the constants γ_i, β_i in the expressions defining $\vec{g}(r)$ and ∇T_0 in (15); specifically, Young takes $\gamma_2 = 0$ but $\gamma_1, \beta_1, \beta_2$ all nonzero. In Chossat's case, the constraint of self-adjointness leads to the degenerate bifurcation problem (24) rather than the simpler problem (22). Of course, a nonself-adjoint perturbation of (24) will in general eliminate this degeneracy. The universal unfolding [6,7] provides a convenient language in which to describe the effect of such perturbations. The universal unfolding of (24) requires only one parameter; one choice is

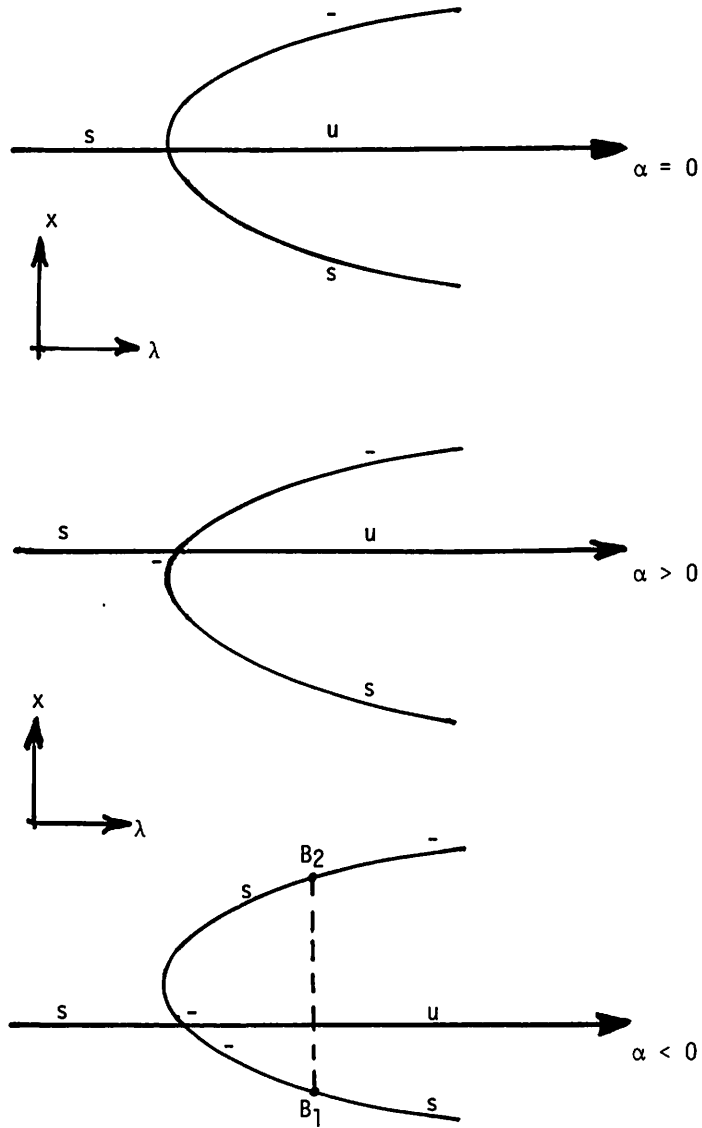


FIG. 14. Perturbations of the organizing center for the symmetric problem.

$$F(z, \lambda; \alpha) = (\varepsilon |z|^2 - \lambda)z + (|z|^2 + C \operatorname{Re} z^3 + \alpha)\bar{z}^2 \quad (26)$$

The universality property means that any sufficiently small perturbation of (24) may be transformed, by an appropriate change of coordinates, to the equation

$$F(z, \lambda; \alpha) = 0 \quad (27)$$

for some value of α . In particular, to determine the qualitative behavior of solutions of perturbations of (24), it suffices to examine (27), a problem involving only one auxiliary parameter.

The bifurcation diagrams

$$\{(z, \lambda) : F(z, \lambda; \alpha) = 0\}$$

which result for $\alpha \neq 0$ are indicated schematically in Fig. 14. The portion shown is the portion contained in the plane $\operatorname{Im} z = 0$; there are two similar pieces in planes rotated 120° and 240° about the λ axis. The branches labeled "u" and "-" are both unstable while those labeled "s" are stable. In addition, when $\alpha < 0$ there is a ring of nonaxisymmetric solutions (shown as a dotted line in the figure) which bifurcates from the axisymmetric solutions at the points B_1 and B_2 . This phenomenon closely resembles the secondary bifurcation discussed by Bauer et al. [1] (see Sec. 4). The nonaxisymmetric solutions are stable or unstable according to $C > 0$ or $C < 0$. If they are stable, then B_2 lies to the left of B_1 in the figure, so that there is an interval in λ where no axisymmetric solutions are stable; if they are unstable B_2 lies to the right of B_1 and there is a short range where two distinct axisymmetric solutions are stable.

The crucial point in our analysis is the following: Although the perturbed versions of (24) involve nonaxisymmetric solutions, neither of the above cases matches Young's data where the nonaxisymmetric and axisymmetric solutions are stable for the same Rayleigh number. This suggests that Young's case is simply not a qualitatively small perturbation of Chossat's. We therefore examined the next few cases on the classification list. Only one of these appears to give agreement with Young's data, namely, a singularity associated

with the vanishing of $f_u(0)$ in (21) where u is the first coordinate of f . Of course, a change of sign of $f_u(0)$ amounts to changing the sign of ϵ in (26); i.e., changing from supercritical bifurcation to subcritical bifurcation. The appropriate perturbed diagram which matches Young's data is shown schematically in Fig. 15 where nonaxisymmetric solutions are again shown by dashed lines. (These lines do not lie in the plane $\text{Im } z = 0$.)

The organizing center of this problem appears to be

$$(|z|^4 - \lambda)z + C(\text{Re } z^3)\bar{z}^2 = 0$$

By the organizing center, we mean the bifurcation problem which results if the external parameters are adjusted so that all singular points on the bifurcation diagram coalesce into a

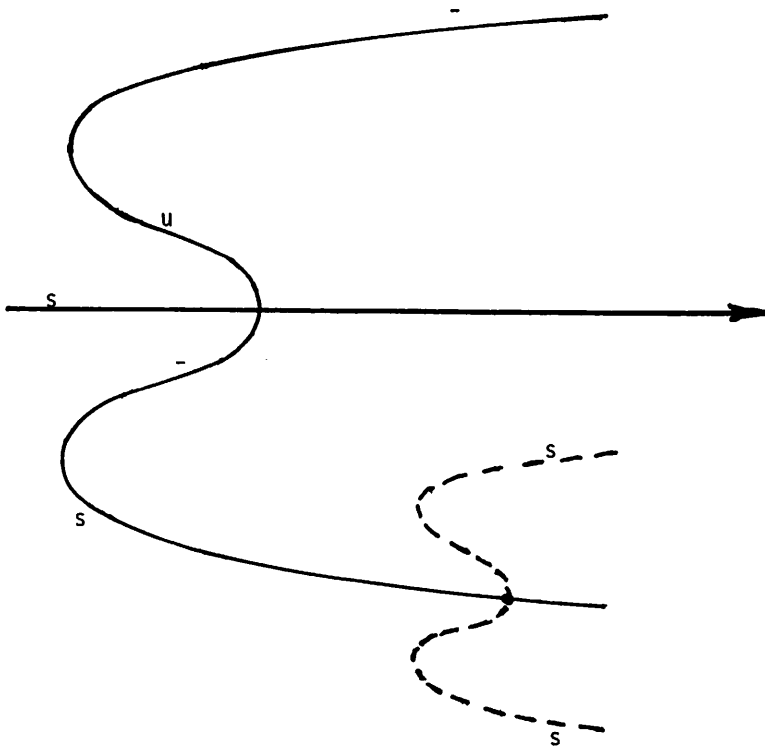


FIG. 15. Bifurcation diagram conjectured to explain Young's numerical results.

single, highly degenerate point. The universal unfolding of the organizing center provides a convenient representation of all bifurcation problems which can result from perturbations. This is rigorously true in a sufficiently small neighborhood, but on a pragmatic level the representation is often valid in a far larger domain than can be a priori justified.

A more detailed analysis of this problem will be published elsewhere [9].

ACKNOWLEDGMENT

This research is sponsored in part by the National Science Foundation grants MCS-7905799 and MCS-7902010.

REFERENCES

1. Bauer, L., Keller, H., and Reiss, E., Multiple eigenvalues lead to secondary bifurcation, *SIAM J. Appl. Math.* 17:101-122 (1975).
2. Chossat, P., Bifurcation and stability of convective flows in a rotating or non-rotating spherical shell, University of Minneapolis, 1978 (preprint).
3. Golubitsky, M., An introduction to catastrophe theory and its applications, *SIAM Review* 20:352-387 (1978).
4. Golubitsky, M., and Keyfitz, B., A qualitative study of the steady-state solutions for a continuous stirred tank chemical reactor, *SIAM J. Math. Anal.* (to appear).
5. Golubitsky, M., Keyfitz, B., and Schaeffer, D., A singularity theory analysis of the thermal chain branching model for the explosion peninsula in the H_2-O_2 reaction (preprint).
6. Golubitsky, M., and Schaeffer, D., A theory for imperfect bifurcation via singularity theory, *Commun. Pure Appl. Math.* 32:21-98 (1979).
7. Golubitsky, M., and Schaeffer, D., Imperfect bifurcation in the presence of symmetry, *Commun. Math. Phys.* 67:205-232 (1979).

8. Golubitsky, M., and Schaeffer, D., An analysis of imperfect bifurcation, *Annals N.Y. Acad. Sci.* 316:127-133 (1979).
9. Golubitsky, M., and Schaeffer, D., The Benard problem in spherical geometry; an example with $O(3)$ symmetry (in preparation).
10. Sattinger, D., Group representation theory and branch points of nonlinear functional equations, *SIAM J. Math. Anal.* 8:179-201 (1977).
11. Schaeffer, D., Qualitative analysis of a model for boundary effects in the Taylor problem, *Proc. Comb. Phil. Soc.* (to appear).
12. Schaeffer, D., and Golubitsky, M., Boundary conditions and mode jumping in the buckling of a rectangular plate, *Commun. Math. Phys.* (to appear).
13. Schaeffer, D., and Golubitsky, M., Bifurcation analysis near a double eigenvalue of a model chemical reaction, *Arch. Rat. Mech.* (to appear).
14. Stein, M., Loads and deformations of buckled rectangular plates, NASA Technical Report R-40, 1959.
15. Uppal, A., Ray, W. H., and Poore, A. B., The classification of the dynamic behavior of continuous stirred tank reactors - Influence of reactor residence time, *Chem. Eng. Sci.* 31:205-214 (1976).
16. Young, R., Finite amplitude thermal convection in a spherical shell, *JFM* 63:695-721 (1974).